Volume 3 no.1 January 1976 Nucleic Acids Research

Chromatin model calculations: Arrays of spherical ν bodies.

R. Douglas Carlson and Donald E. Olins

University of Tennessee-Oak Ridge Graduate School of Biomedical Sciences and the Biology Division, Oak Ridge National Laboratory, Oak Ridge, TN 37830, USA

Received 20 October 1975

ABSTRACT

Chromatin fibers consist of globular nucleohistone particles (designated ν bodies) along the length of the chromatin DNA with approximately 6- to 7-fold compaction of the DNA within the ν bodies. We have calculated theoretical small-angle x-ray scattering curves and have compared these with experimental data in the literature. Several models predict maxima at the correct angles. The first maximum (~110 Å) results from interparticle interference, while both the spatial arrangement and the structure factor of the ν bodies can contribute to the additional small-angle maxima. These calculations suggest models which can account for the electron microscopic observation that chromatin is seen as either ~100- or ~200- to 250-Å-diameter fibers, depending on the solvent conditions. They also account for the limited orientability of the x-ray pattern from pulled chromatin fibers.

INTRODUCTION

The x-ray diffraction patterns from unoriented gels of whole nuclei or isolated chromatin and from oriented chromatin fibers show a series of low-angle rings[1–3]. Several models have been proposed to explain the x-ray data[1–9], the most widely accepted ones having the chromatin fiber in a supercoiled conformation, with the double-stranded DNA constrained into a continuous helix by the histones[5–7]. Theoretical calculations for regular and polyhelical models exhibit x-ray maxima very near the observed angles and show that no unique helix parameters can be determined from the x-ray data alone[6–8].

Ultrastructural studies have demonstrated that chromatin can take the form of ~100- and ~200- to 250-Å-diameter fibers, depending upon solvent conditions[10–18]. Recent evidence suggests that chromatin consists of globular nucleohistone particles (ν bodies) connected by DNA, much like beads on a string[19–36]. These particles have been observed by electron microscopy in spread chromatin from a variety of

© Information Retrieval Limited 1 Falconberg Court London W1V 5FG England

eucaryotes using different staining and shadowing techniques[19–21, 23, 26]. In our laboratory electron microscopic studies of isolated monomer particles prepared by either endonuclease digestion or sonication have shown that these particles closely resemble the ν bodies observed in the intact fibers, both in size and in general appearance[37].

The observed beads-on-a-string conformation is inconsistent with a superhelical model. We have, therefore, investigated the possibility that a periodic arrangement of the chromatin ν bodies may be responsible for the small-angle x-ray reflections[22, 27, 33, 35]. We have systematically calculated the scattering by many different arrays of ν bodies and have compared these model calculations with published x-ray data[4, 6]. No single particle array uniquely accounts for the x-ray data. Nevertheless, certain linear arrays do give the x-ray maxima and also have fiber diameters[10–18] and DNA packing ratios[22, 31, 34, 36] consistent with published values.

MODELS

We have calculated the spherically averaged x-ray scattering by linear and flexible strings of spheres, by different helical arrays, and by different three-dimensional close-packing arrays. Since almost nothing is known about the internal structure of an individual ν body [i.e., the three-dimensional electron density distribution $\rho(r, \theta, \varphi)$], we have used spherically symmetric electron density distributions $\rho(r)$ to represent them. In most calculations we have used uniform-density spheres [$\rho(r)$ = constant], but we have also investigated the effect of nonuniform density on the calculations by trying several other electron density distributions: a core of one density surrounded by a shell of another; a core of one density surrounded by two shells; a linearly increasing or decreasing density out to a radius R; and a cosine density, [$\rho(r) = \cos(\pi r/2R)$]. Scattering by the connecting DNA has been ignored. Even such naive approximations should give information about the structure of chromatin at the interparticle level.

It is conventional to describe a discontinuous helix in terms of an axial rise or unit height h (translation per subunit along the helix axis) and an angular separation or unit twist t (angle of rotation per subunit about the helix axis)[38]. A helix of spheres of diameter d, with helix parameters h and t, is unique when the outside diameter D of the helix (twice the distance from the axis to the center of a sphere plus d) is specified. The handedness of the helix makes no difference in these calculations. Because we are concerned about the inter-subunit contacts which would stabilize

such helical arrays, we have found it "visually" informative to further categorize them according to the number of other subunits with which each is in contact (0, 2, 4, or 6). Equation 5 and Table 1 of a paper by Erickson[39] have been used to calculate the positions of spheres in 4- and 6-contact helices respectively. Helices with no contacts between spheres would not be stable and have not been considered.

The following classes of linear particle arrays have been considered:

Linear Strings (Fig. 1a). A periodic linear array of touching spheres.

Flexible Strings (Fig. 1b). The amount of flexibility is defined by the angles α and ψ which are randomly generated for each sphere. If a straight line is drawn through the centers of two adjacent spheres (1 and 2), the line through the centers of spheres 2 and 3 will form an angle α with the extension of the first line ($-\alpha_{max} < \alpha < \alpha_{max}$). The angle ψ is a torsion angle and has a value between 0 and 2π radians. A linear string results when $\alpha_{max} = 0°$. Because the α's and ψ's were randomly generated, the calculations were repeated several times for each α_{max}.

2-Contact Helices (Fig. 1c). These are open helices with each sphere in contact with only the two neighbor spheres along the strand. As long as spheres do not overlap, any three of the four variables (h, t, d and D) are independent. There is no stabilization arising from interactions of spheres other than those interactions between covalently linked neighbors.

4-Contact Helices (Fig. 1d). Each sphere is in contact with spheres above and below as well as with adjacent spheres along the strand. According to the notation of Erickson[39] these would correspond to the (1, n) helices with n = 2,3,4, etc. For each

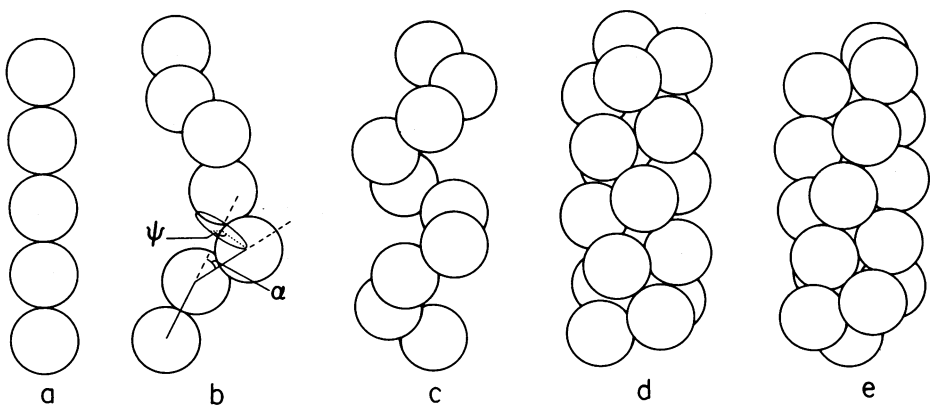

Figure 1. Linear arrays of spheres: (a) linear string; (b) flexible string; (c) 2-contact helix; (d) 4-contact (1,4) helix; (e) 6-contact (1,3,4) helix.

n there is a range of allowable values of t. Only two of the four variables described above are independent. Integer helices are special cases in which the two stabilizing contacts are directly above and below. Thus a (1, 4) helix with a unit twist of 90° is an integer helix with 4 spheres per helical turn.

6-Contact Helices (Fig. 1e). This class represents the tightest structures of all the helices. The spheres are hexagonally packed on the surface of the helix, each sphere being in contact with six other spheres. Erickson[39] calls these (1, m,n) helices, where m and n are integers limited by the previously described constraints to be: m= 2,3,4, etc. and n = m + 1. For a given sphere size and integer m, the helix parameters are unique.

In considering the ways in which spheres could pack, we have also considered the possibility that there are regions of close-packed ν bodies. Such close-packing might be possible in gels, where the individual chromatin fibers are flexible and randomly oriented; in pulled fibers, where the individual chromatin fibers are arranged in partially parallel arrays; and in pellets of close-packed monomer ν bodies. We have calculated the spherically averaged diffraction from the following three-dimensional close-packing arrays: cubic close-packing, face-centered close-packing, body-centered cubic close-packing, and hexagonal close-packing[40].

CALCULATIONS

The spherically averaged scattering of x rays by a model structure made up of N identical spherically symmetrical subunits can be calculated using the appropriate form of the Debye expression[41].

$$I(h) = F^2(h) \sum_m \sum_n \frac{\sin h\, r_{mn}}{h\, r_{mn}} \qquad [1]$$

where $F(h)$ is the structure factor of a subunit; r_{mn} is the separation distance between the centers of the mth and the nth subunits; and $h = (4\pi/\lambda) \sin\theta$. Here λ is the x-ray wavelength and 2θ is the scattering angle between the incident and scattered x rays.

For a spherically symmetrical subunit of radius a with an electron density $\rho(r)$, the structure factor is

$$F(h) = \int_0^a \rho(r) \frac{\sin h\, r}{h\, r}\, 4\pi r^2\, dr \qquad [2]$$

Evaluating [2] for a uniform density sphere containing N_e effective scattering electrons, one obtains[42]

$$F(h) = 3N_e \frac{\sin(ha) - ha\cos(ha)}{(ha)^3} . \qquad [3]$$

In a similar manner, equations for $F(h)$ were derived using [2] for other model electron densities.

These calculations were made on a PDP 11/20 computer using an on-line Tektronix graphics display to plot the theoretical curves. To calculate the scatter by a helix of uniform density spheres of diameter d, for example, the parameters h, t and D were used to generate the positions of all the spheres. The values of r_{mn} were then calculated and used to evaluate [1] for each h, using the corresponding $F(h)$ which had previously been calculated using [3] and stored in memory. For each model, the intensities were calculated and plotted at increments of $2\theta = 0.5$ mradians.

RESULTS

Based on our calculations, the following general statements can be made: (a) For several quite different arrays based on ~110-Å-diameter spherically symmetric particles, x-ray maxima are predicted at positions in agreement with the experimental positions. (b) The first maximum is due to the periodic arrangement of these particles. It occurs at an equivalent Bragg spacing approximately equal to the principal interparticle distance. The additional small-angle maxima reflect both this periodicity and the particle structure factor, the latter being dominant. (c) Both the diameter of the spheres and the principal interparticle distance must be ~110 Å to have all of the maxima in the correct positions. (d) For all of these models based on regular arrays of uniform electron density spheres, the calculated relative intensities fall off more quickly with each Bragg angle, than do published experimental data. To improve the agreement it is necessary to use spheres with nonuniform electron-density distributions. These points will be discussed in more detail below. Several selected model calculations are presented in Fig. 2, and a partial summary of the calculations is shown in Table 1.

The calculated x-ray scattering by linear strings of touching 110-Å spheres of two different $\rho(r)$'s is shown in Fig. 2b. Maxima are predicted at approximately the

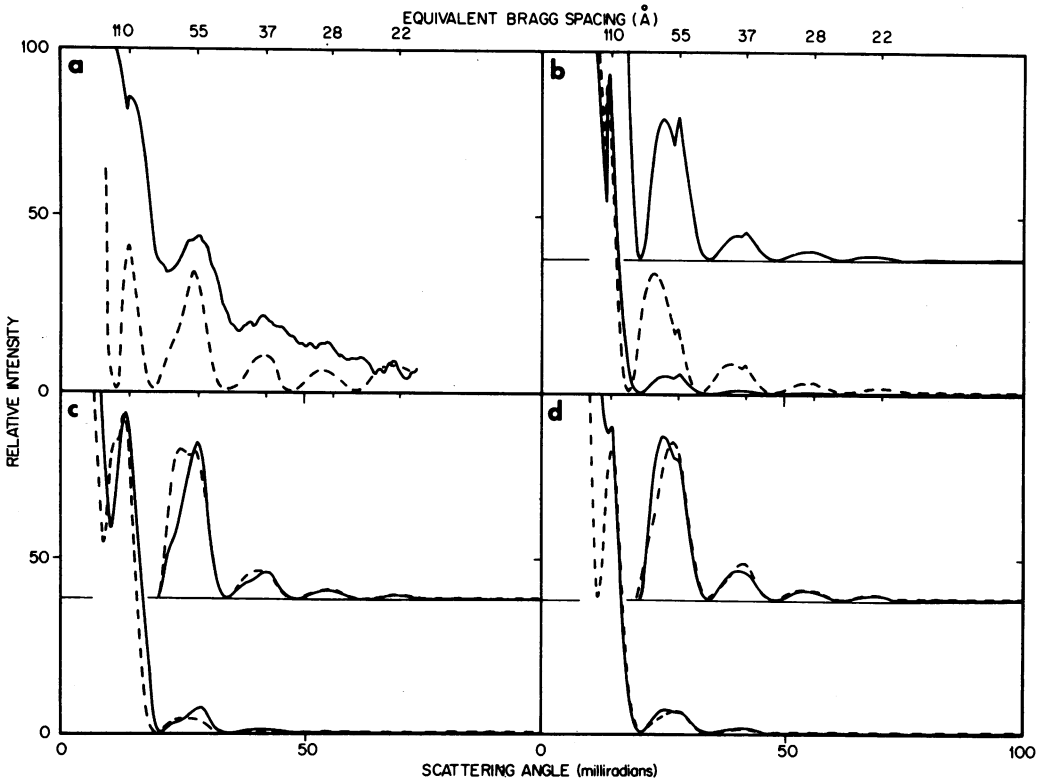

Figure 2. Theoretical x-ray diffraction by model arrays of 110-Å-diameter spheres, compared with experimental data. (a) Data from Subirana et al.[4] which has not been corrected for instrumental and solvent scatter (solid line), and from Pardon and Wilkins[6] which those authors corrected by subtracting a smooth background so that the intensities at the troughs are zero (dashed line). (b) Linear strings of uniform-density spheres (solid line), and spheres with two shells surrounding the core (core: $r = 10$ Å, $\rho = 1.5$; shell 1: $r = 40$ Å, $\rho = 1.0$; shell 2: $r = 55$ Å, $\rho = 3.0$) (dashed line). In addition, a magnified portion of the solid curve which has had the relative intensity multiplied by a constant to better show the maxima at larger angles is shown on a raised abscissa. (c) A (1,2,3) helix (solid line) and a (1,3) helix with h = 35.0 Å and t = 110° (dashed line). Magnified portions of both curves are shown. (d) A flexible string with α_{max} = 30° (solid line) and a small (19 spheres) domain of hexagonally close-packed spheres (dashed line). Magnified portions of both curves are shown. Arrays of 20 uniform-density spheres were used for all calculations unless otherwise indicated. Longer arrays do not appreciably alter the relative intensities. The curves were adjusted to approximately the same intensity for the ~110-Å peak, or in the case of the magnified curves, for the ~55-Å peak.

correct Bragg angles. The ~110-Å maximum, as is observed experimentally, is narrower than the other maxima. The splitting of the wider-angle maxima results from the sharp modulation of $F^2(h)$ in [1] by the lattice term (the double sum) for a linear string. These and additional calculations using other $\rho(r)$'s for different arrays show that the relative intensities of the maxima can be greatly affected by the electron density distribution within the spheres. Calculations for flexible strings show that both the first maximum and the lattice contribution to the other maxima become less pronounced as the flexibility increases. The scatter for a flexible string of spheres with $\alpha_{max} = 30°$ is shown in Fig. 2d. By $\alpha_{max} = 40°$, the ~110-Å maximum has disappeared.

TABLE 1. Calculated parameters for certain linear arrays of 110-Å spheres

Model	Fiber diameter, D (Å)	Unit height, h (Å)	Unit twist, t (°)	DNA packing ratio*	Correct spacings?†
Linear string	110	110	—	6.4	Yes
Flexible string (α_{max} = 0–30°)	110	110‡	—	6.4‡	Yes
Helix models					
2-Contact	220	46.5	130	15.1	Yes
	220	77.8	90	9.0	No
	250	48.0	90	14.6	No
4-Contact					
(1,2)	205–225	55.0–34.8	180.0–131.8	13.7–20.1	Some§
(1,3)	225–250	34.8–25.8	131.8– 97.7	20.1–27.1	Yes
(1,4)	250–283	25.8–20.5	97.7– 77.4	27.1–34.1	Some§
6-Contact					
(1,2,3)	225	34.8	131.8	20.1	Yes
(1,3,4)	250	25.8	97.7	27.1	Yes
(1,4,5)	283	20.5	77.4	34.1	No

*The DNA packing ratio along the fiber is calculated assuming 700 Å of DNA/110-Å-diameter sphere.

†Experimental data show that maxima occur at equivalent Bragg spacings of ~110, 57, 37 Å, etc.[6,7,21].

‡Following along the flexible string.

§Some of the helices within this class give the correct spacings.

Certain 2-, 4-, and 6-contact helices of 110-Å spheres also give maxima at the proper positions. We consider the 2-contact helices to be the least likely to exist since there are no stabilizing interactions along the helix axis (see Fig. 1c). Because the possible combinations of helix parameters are unlimited, we have only considered 2-contact helices with $D < 300$ Å. The results of several representative 2-contact calculations, one of which gives maxima at the correct spacings are shown in Table 1. A certain 2-contact helix of spherical ν bodies with helix parameters $h = 60$ Å, $t = 43.3°$, $d = 100$ Å and $D = 370$ Å was recently proposed to explain neutron-scattering data at very small angles[43]. The possible presence of x-ray maxima in this angular region is of considerable interest, but our calculations over the entire angular range show that this particular model does not give the ~110-Å maximum.

The 4- and 6-contact helices would be more stable. The entire range of helix parameters which includes helix diameters similar to experimentally observed fiber diameters was covered. Fig. 2c shows the results of calculations for a (1,3) helix (4-contact) and a (1,2,3) helix (6-contact). Both give maxima at the correct positions and a maximum at ~110-Å that is somewhat narrower than the rest. It should be noted that these are very similar structures. In general, 4- and 6-contact helices only give the correct maxima when t is between ~95 and 140°. These include certain (1,2) and (1,4) helices as well as the (1,3) helices, and the (1,2,3) and (1,3,4) helices. The helix parameters for these structures are shown in Table 1.

Calculations for several close-packed arrays of spheres show that they too can give the small-angle maxima, but only if the ordered domains are small. Fig. 2d shows the scatter by a small domain of hexagonally close-packed spheres. Similar agreement is observed for small domains (~20 spheres) of other close-packing arrays. These small clusters of spheres have diameters less than 4 times the diameter of a single sphere. Splitting and shifting of maxima occur as the sizes of these domains are increased, and become quite pronounced for clusters of ~80 spheres or more. Thus, if there are ordered regions of close-packed ν bodies in a gel or fiber of chromatin, these regions must be small.

The calculations shown in Fig. 2 and in Table 1 are for arrays of touching 110-Å-diameter spheres. Whenever the sphere diameter is reduced while the interparticle spacing is unchanged, there is a proportional shift in all of the maxima but that at ~110 Å. When smaller spheres are touching, all of the maxima are shifted.

DISCUSSION

A comparison of the model calculations and small-angle x-ray data such as those shown in Fig. 2 must be viewed with an awareness of the following limitations: (a) We have compared unoriented model curves with data from oriented chromatin, as have several other researchers[6,7,9]. While only the ~110-Å ring shows more than very weak meridional orientation in such samples[44], the theory used assumes no orientation and is thus not rigorously applicable. (b) These experimental data have not been quantitatively corrected for both solvent and background scatter. Such corrections would affect the intensities of the maxima, but not their positions. (c) There may be considerable conformational heterogeneity in chromatin. For example, if only a portion of the ν bodies were in an ordered array, the relative intensity of the ~110-Å maximum would be reduced. (d) Our calculations suggest that the electron density distribution within the ν body is an important consideration. The relative intensities of the maxima are much closer to the experimental values when the electron density is highest near the outside of the sphere, as is the case for the core-shell-shell density used in Fig. 2b. There is in fact some experimental evidence that much of the DNA, which has a higher effective electron density than protein, is located on the exterior of the ν body[32]. We have, nevertheless, chosen to show in Fig. 2 primarily model calculation made using uniform-density spheres because so little is known about the actual structure of the ν body.

The agreement in the positions of the maxima is good, and the lack of agreement in the relative intensities may be due to the above factors. We therefore suggest that a regular array of ν bodies is responsible for the x-ray data. No single array is uniquely consistent with those data, however, several seem preferable when additional data are considered.

These calculations suggest that the ~110-Å peak arises solely from the particle array and that the particle structure factor makes the dominant contribution to the other maxima. A recent neutron-scattering study has likewise indicated that only the ~110-Å maximum is primarily attributable to the particle array[45]. This explains why the ~110-Å ring can be strongly oriented along the meridian in pulled fibers when the other rings are only slightly oriented. The presence of some orientation suggests that the particle array is either a string or helix.

Ultrastructural studies have shown that chromatin fibers can have various widths

depending upon solvent conditions. Thin sections of water-swollen nuclei[15–17], or chromatin spread on an aqueous hypophase containing a chelating agent and then dried and stained[16], yield fiber widths of ~100 Å. The disruptive effects of organic solvents[46] may explain the lack of visualization of ν bodies in these experiments[21]. We suggest, that at low ionic strength and in the absence of divalent metal ions, chromatin fibers consist of linear or flexible strings of "touching" ν bodies. The DNA packing ratio in the fiber would be ~6–7/1[20, 22, 31, 33, 34, 36].

Thin sections of nuclei with condensed chromatin[12, 17], or chromatin spread on a hypophase and then dried and stained[10, 11, 14, 16, 18], yield fiber widths of ~200–250 Å. Several helical arrays of ν bodies could account for the 200- to 250-Å chromatin fiber. Golumb and Bahr[18] have measured the DNA packing ratio in the ~200-Å chromatin fiber obtained from human mitotic chromosomes to be 28.3/1. Table 1 indicates the expected DNA packing ratios for different models. The (1,2,3), (1,3,4) and (1,3) helices come reasonably close to satisfying the constraints of both fiber diameter and DNA packing ratio. Recent electron micrographs of freeze-fractured developing spermatocytes suggest to us a possible helical arrangement of particles in the chromatin fibers[47]. Both right- and left-handed helical regions are observed. Shadowing a helix of spherical particles from different directions relative to the fiber axis could preferentially enhance either right- or left-handed helical structure.

These calculations suggest spherical ν-body diameters of ~110 Å. Our electron microscopic studies, however, have indicated that the dehydrated ν bodies along the fiber have a diameter of 60–80 Å and that isolated ν bodies have a diameter of ~80 Å[19–21, 37]. We have previously stated our belief that the diameter of the hydrated ν bodies is likely to be greater than 60–80 Å and have pointed out that the volumes of ribosomes calculated from electron microscopic measurements are about 50% of the volumes measured by hydrodynamic techniques[48]. Oudet et al.[36] have recently observed ν-body diameters of ~130 Å following platinum shadowing of the spread, unfixed chromatin preparations. We wish to point out that it is exceedingly difficult to determine accurately the proportionate increase in diameter that would result from the platinum deposition. Clearly, definitive hydrodynamic and light- or x-ray-scattering data on isolated particles are more reliable measures of ν-body diameter than techniques which variously involve fixation, dehydration, shadowing, and difficult calibration. If the ν bodies do shrink to ~80 Å in diameter during dehydration and yet maintain their ordered array, our calculations predict a shift in the maxima.

Such a shift has been seen in chromatin fibers at <75% relative humidity, where maxima occur at ~75 and 38 Å [3, 6, 8].

It is clear that a continuous superhelix is not necessary to explain the x-ray data. This is further supported by the observation that monomer ν bodies (isolated after either sonication or micrococcal nuclease digestion of isolated nuclei, made 5 mM $MgCl_2$, and pelleted in the ultracentrifuge) give the normal small-angle x-ray pattern (Olins, A. L., Breillat, J. P., Carlson, R. D., Senior, M. B., and Olins, D. E., manuscript in preparation). Whether this is due to a partially ordered close packing of ν bodies or whether they associate into linear or helical arrays is not clear. We have observed, using both light and electron microscopy, that they do form fibrous aggregates in the presence of Mg^{2+}. We are presently using x-ray scattering to study both the structure and associative properties of the monomer ν bodies.

ACKNOWLEDGMENTS

We gratefully acknowledge Drs. J. R. Einstein, R. W. Hendricks, R. W. Erickson, A. L. Olins, and M. B. Senior, for helpful discussions and criticisms. This research was sponsored by the U.S. Energy Research and Development Administration under contract with the Union Carbide Corporation, by National Institute of General Medical Science research grant GM19334 to D.E.O., and by National Institute of General Medical Science postdoctoral fellowship GM55247 to R.D.C.

REFERENCES

[1]Wilkins, M. H. F. (1956) Cold Spring Harbor Symp. Quant. Biol. 21, 75–90
[2]Luzzati, V. and Nicolaieff, A. (1959) J. Mol. Biol. 1, 127–133
[3]Wilkins, M. H. F., Zubay, G. and Wilson, H. R. (1959) J. Mol. Biol. 1, 179–185
[4]Subirana, J. A., Puigjaner, L. C., Roca, J., Llopis, R. and Suau, P. (1974) in The Structure and Function of Chromatin, (Fitzsimons, D. W. and Wolstenholme, G. E. W., eds.), pp. 157–179, Elsevier, New York
[5]Pardon, J. F., Wilkins, M. H. F. and Richards, B. M. (1967) Nature 215, 508–509
[6]Pardon, J. F. and Wilkins, M. H. F. (1972) J. Mol. Biol. 68, 115–124
[7]Subirana, J. A. and Puigjaner, L. C. (1974) Proc. Natl. Acad. Sci. USA 71, 1672–1676
[8]Pardon, J. F., Richards, B. M. and Cotter, R. I. (1973) Cold Spring Harbor Symp. Quant. Biol. 33, 75–81
[9]Bram, S. and Ris, H. (1971) J. Mol. Biol. 59, 304–317
[10]DuPraw, E. J. (1965) Nature (London) 206, 338–343

[11]Gall, J. G. (1966) J. Ultrastruct. Res. 19, 382–397
[12]Davies, H. G. (1968) J. Cell Sci. 3, 129–150
[13]Everid, A. C., Small, J. V. and Davies, H. G. (1970) J. Cell Sci. 7, 35–48
[14]Wolfe, S. L. and Grim, J. N. (1967) J. Ultrastruct. Res. 19, 382–397
[15]Brasch, K., Seligy, V. L. and Setterfield, G. (1971) Exp. Cell Res. 65, 61–72
[16]Ris, H. and Kubai, D. F. (1970) Annu. Rev. Genet. 4, 263–294
[17]Olins, D. E. and Olins, A. L. (1972) J. Cell Biol. 53, 437–455
[18]Golumb, H. M. and Bahr, G. F. (1974) Chromosoma 46, 233–245
[19]Olins, A. L. and Olins, D. E. (1973) J. Cell Biol. 59, 252a
[20]Olins, A. L. and Olins, D. E. (1974) Science 183, 330–332
[21]Olins, A. L., Carlson, R. D. and Olins, D. E. (1975) J. Cell Biol. 64, 528–537
[22]Senior, M. B., Olins, A. L. and Olins, D. E. (1975) Science 187, 173–175
[23]Woodcock, C. L. F. (1973) J. Cell Biol. 59, 368a
[24]Rill, R. and Van Holde, K. E. (1973) J. Biol. Chem. 248, 1080–1083
[25]Sahasrabuddhe, C. G. and Van Holde, K. E. (1974) J. Biol. Chem. 249, 152–156
[26]Van Holde, K. E., Sahasrabuddhe, C. G., Shaw, B. R., van Bruggen, E. F. J. and Arnberg, A. C. (1974) Biochem. Biophys. Res. Commun. 60, 1365–1370
[27]Van Holde, K. E., Sahasrabuddhe, C. G. and Shaw, B. R. (1974) Nucleic Acids Res. 1, 1579–1586
[28]Oosterhof, D. K., Hozier, J. C. and Rill, R. L. (1975) Proc. Natl. Acad. Sci. USA 72, 633–637
[29]Hewish, D. R. and Burgoyne, L. A. (1973) Biochem. Biophys. Res. Commun. 52, 504–510
[30]Burgoyne, L. A., Hewish, D. R. and Mobbs, J. (1974) Biochem. J. 143, 67–72
[31]Noll, M. (1974) Nature 251, 249–251
[32]Noll, M. (1974) Nucleic Acids Res. 1, 1573–1578
[33]Kornberg, R. D. (1974) Science 184, 868–871
[34]Griffith, J. D. (1975) Science 187, 1202-1203
[35]Carlson, R. D., Olins, A. L. and Olins, D. E. (1975) Biochemistry 14, 3122–3125
[36]Oudet, P., Gross-Bellard, M. and Chambon, P. (1975) Cell 4, 281–300
[37]Olins, A. L., Senior, M. B. and Olins, D. E., J. Cell Biol., in press
[38]IUPAC-IUB Commission of Biochemical Nomenclature (1971) Biochem. J. 121, 577–585
[39]Erickson, R. W. (1973) Science 181, 705–516
[40]Patterson, A. L. and Kasper, J. S. (1959) in International Tables for X-Ray Crystallography, Vol. II (Kasper, J. S. and Lonsdale, K., eds.), pp. 342–354, Kynoch Press, Birmingham, England
[41]Debye, P. (1915) Ann. Physik. 46, 809–823
[42]Rayleigh, Lord (1914) Proc. Roy. Soc. London, Ser. A 90, 219–225
[43]Bram, S., Butler-Browne, G., Baudy, P. and Ibel, K. (1975) Proc. Natl. Acad. Sci. USA 72, 1043–1045
[44]Richards, B. M. and Pardon, J. F. (1970) Exp. Cell Res. 62, 184–196
[45]Baldwin, J. P., Boseley, P. G., Bradbury, E. M. and Ibel, K. (1975) Nature (London) 253, 245–249
[46]Pooley, A. S., Pardon, J. F. and Richards, B. M. (1974) J. Mol. Biol. 85, 533–549
[47]Henley, C. (1973) Chromosoma 42, 163–174
[48]Hill, W. E., Rossetti, G. P. and Van Holde, K. E. (1969) J. Mol. Biol. 44, 263–277